

RESEARCH ARTICLE

View Article Online
View Journal

Cite this: DOI: 10.1039/d5qi01994j

A crystalline chiral phosphide for the synthesis of the first P-stereogenic P(III) fluoride: a stable ligand for the Rh-catalyzed asymmetric arylation of isatins

Laila Al Baridi, Giorgio Parla, Alberto Herrera,* Frank W. Heinemann and Romano Dorta *

Received 29th September 2025,
Accepted 26th November 2025

DOI: 10.1039/d5qi01994j

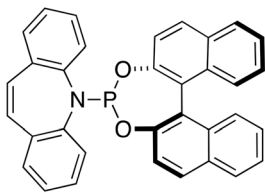
rsc.li/frontiers-inorganic

Introduction

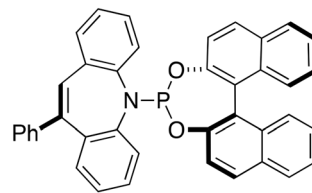
Despite the fact that Burg and Brendel 66 years ago reported the synthesis of the first organo-fluorophosphine, namely $(CF_3)_2PF$,¹ the use of P(III) fluorides as ligands in coordination chemistry is, apart from PF_3 ,² scarcely described.³ Applications in catalysis are even rarer,⁴ and asymmetric versions have not yet been reported, due to the lack of effective synthetic methods towards optically pure fluorophosphines. Chiral phosphines are the ligands of choice for many transition-metal-catalyzed asymmetric reactions in industry and academia.⁵ Of special interest are P-stereogenic phosphines, which place chirality in proximity of the metal center. This concept gained industrial maturity with Monsanto's L-Dopa process in the late 1970's, for which Knowles was awarded the Nobel prize.⁶ However, the synthesis of enantiopure P-stereogenic compounds is notoriously difficult⁷ and a topic of high relevance to asymmetric catalysis.⁸ In particular, the stereoselective installation of a P-F bond in

P-stereogenic phosphine ligands has remained elusive so far and is of prime interest because it would allow to introduce strong steric and electronic differentiation on the P-donor and considerably widen the diversity of chiral ligand design.⁹ Even though the P-F bond is polar and possesses a significant strength of 545 kJ mol⁻¹,¹⁰ applications of fluorophosphines in catalysis have been hampered by their high propensity towards redox disproportionation.⁴

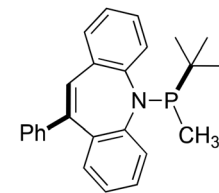
In a recent evolution of the 'privileged ligand'¹¹ we found the planar chirality in the diastereomers (pS,R)-2 and (pR,R)-2 to completely overwhelm the axial chirality of the potent binol auxiliary in the enantioselective Hayashi-Miyaura reaction.¹² Some years ago, we explored the possibility to introduce the promising P-chiral *tert*-butylmethylphosphine function¹³ to such systems by isolating the stereochemically stable ligand *rac*-3.¹⁴ Having taken inspiration from the seminal reports on P-stereogenic P(III)-fluorides by Wild,¹⁵ Pringle,^{4b} Puckette,^{4e} and others,¹⁶ we dis-



(R)-1



(pS,R)-2

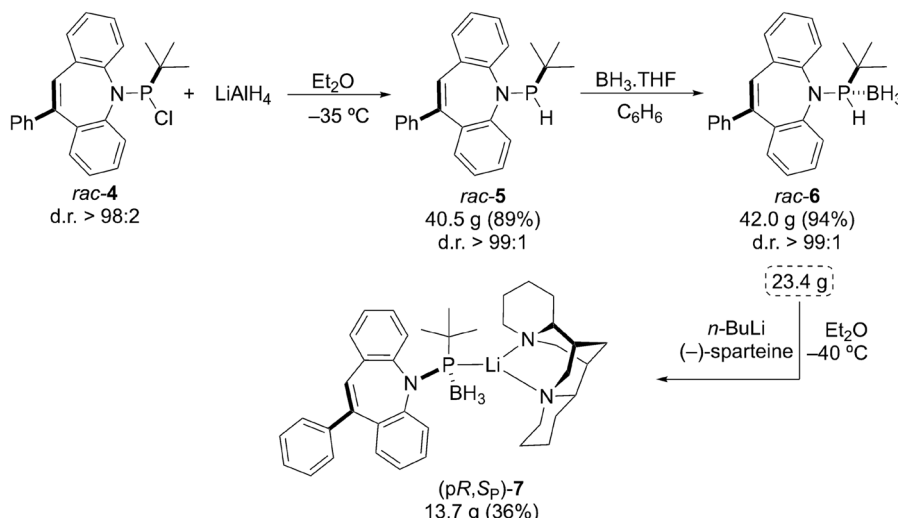


rac-3

Department Chemie und Pharmazie, Anorganische und Allgemeine Chemie, Friedrich-Alexander-Universität Erlangen-Nürnberg, Egerlandstraße 1, 91058 Erlangen, Germany. E-mail: romano.dorta@fau.de

close here a perfectly stereoselective P-F bond forming protocol that allowed us to isolate the first enantiopure P-stereogenic P(III) fluoride, its Rh(I) complex, and use in catalytic asymmetric C-C bond formation.





Scheme 1 Synthetic route to the enantiopure crystalline phosphide (pR,S_P)-7.

Results and discussion

We opted for Livinghouse's protocol for the synthesis of optically pure P-stereogenic phosphines *via* chiral phosphide intermediates obtained by enantioselective deprotection of secondary phosphine-boranes, which then are quenched with organic electrophiles.¹⁷ In our case, the diastereomerically pure, BH_3 -protected, secondary phosphinamide **rac-6** (Scheme 1) is prepared by reducing diastereomerically enriched (d.r. > 98 : 2) chlorophosphine **rac-4** with LiAlH_4 to almost diastereopure **rac-5** followed by protection with $\text{BH}_3\text{-THF}$. Deprotonation of 23.4 g of **rac-6** with the $n\text{-BuLi}/(-)\text{-sparteine}$ mixture in Et_2O at $-40\text{ }^\circ\text{C}$, yields 13.7 g of phosphide (pR,S_P)-7. Non-decoupled NMR spectra of the ^{31}P , ^{11}B , and ^7Li nuclei display multiplets centered at 96.5, 31.6, and 0.8 ppm, respectively. The molecular mass for 7, estimated by DOSY-NMR (585 g mol⁻¹) corresponds to a monomer (MW = 612 g mol⁻¹). Single crystals of 7 grow from 1,2-difluorobenzene/ Et_2O and XRD analysis confirms its absolute configuration and monomeric structure featuring a P–Li bond (see Fig. 1) contrasting Livinghouse's chiral phosphide, in which the borane moiety bridges the Li-sparteine complex.¹⁸ Unlike Livinghouse's dynamically resolving system, we think that in our case the BuLi/sparteine deprotection enables resolution of the lithium phosphide sparteine complex by diastereoselective crystallization¹⁹ from cold Et_2O solutions, which might explain the modest yields of (pR,S_P)-7. The (pS,R_P)-antipode is accessible by using (+)-sparteine (see the SI for details).

With optically pure phosphide (pR,S_P)-7 in hand we first validated its utility as a stereospecific nucleophile for the synthesis of our well-understood P-alkene **rac-3** since earlier attempts of stereospecific C–N bond formation between lithium phenyl-dibenzooazepinate²⁰ and enantiopure (*R*)-(Me)(*t*Bu)PBr(BH_3) (Imamoto's method)²¹ only afforded **rac-3** albeit in diastereomerically pure form. Gratifyingly, methyl iodide reacts smoothly with (pR,S_P)-7 to produce the protected phosphinamide (pR,R_P)-8 in 99% ee (Scheme 2), which is deprotected to (pR,R_P)-3 by

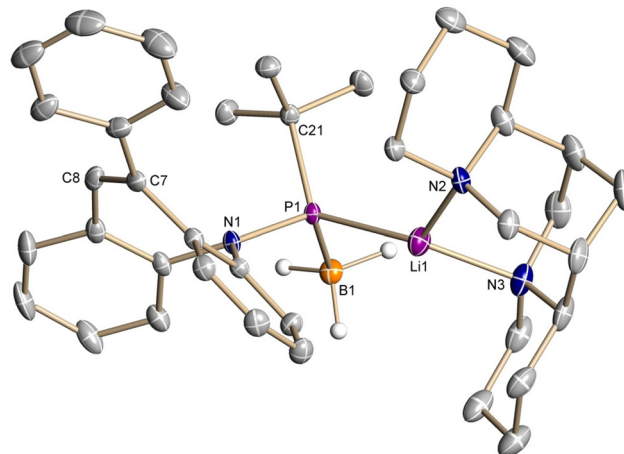
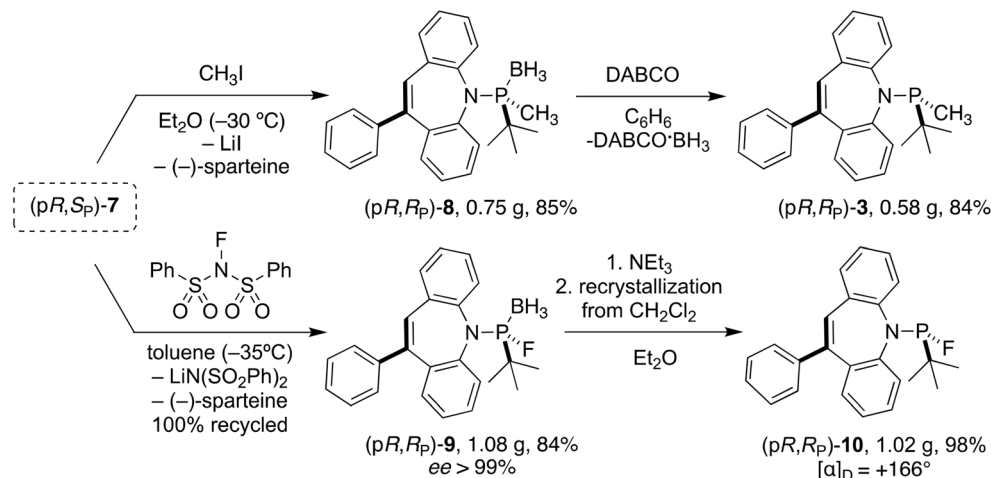
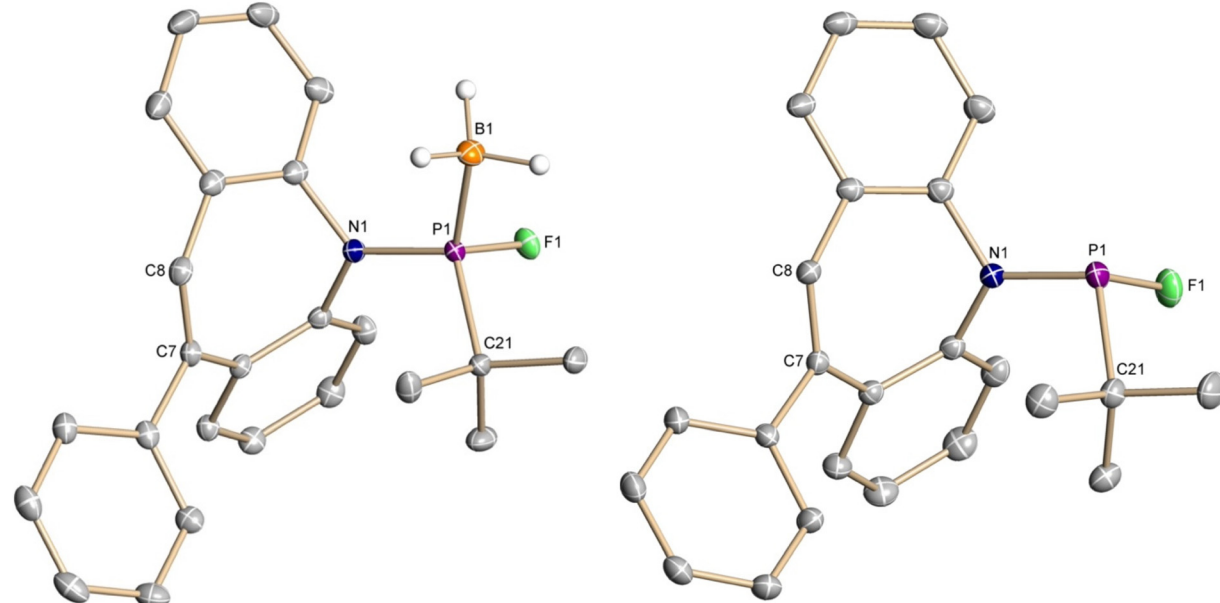


Fig. 1 Crystal structure of (pR,S_P)-7 (50% displacement ellipsoids, most H atoms are omitted). Selected distances (Å) and angles (deg): Li1–P1 2.488(3), Li1–N2 1.995(4), Li1–N3 2.024(4), P1–B1 1.956(2), P1–N1 1.7469(15), P1–C21 1.8790(17), C7–C8 1.355(3), N1–P1–Li1 106.06(10), C21–P1–Li1 121.50(10), N1–P1–C21 112.88(9), N1–P1–C21 103.46(7).

DABCO. Its precise stereochemistry is established by the crystal structure of the Rh(i) complex **11** (see below and Fig. S1).

Likewise, phosphide (pR,S_P)-7 reacts with *N*-fluorobenzene-sulfonimide²² with retention of configuration at phosphorous to the BH_3 -protected diastereopure and enantiopure amido-*t*-butyl fluorophosphine (pR,R_P)-9 (Scheme 2).²³ P–F bond formation is evident in $^{31}\text{P}\{^1\text{H}\}$ and non-decoupled ^{19}F NMR spectra, which show a doublet of multiplets and a doublet of quartets centered at 155.9 ($J_{\text{PF}} \approx 1050$ Hz) and -109.4 ppm ($J_{\text{FP}} \approx 1050$ Hz, $J_{\text{FH}} = 16.1$ Hz), respectively (Fig. S26). The ^1H NMR spectrum shows a doublet at 1.09 ppm and broad multiplets between 0.45–0.26 ppm corresponding to the *t*Bu and BH_3 moieties. Enantiopurity was confirmed by chiral HPLC (Fig. S41 in the SI). Fig. 2 shows the crystal structure of (pR ,



Scheme 2 Syntheses of enantiopure (pR,R_p) -3 and fluorophosphinamide (pR,R_p) -10.Fig. 2 Crystal structures of (pR,R_p) -9 and (pR,R_p) -10 (50% displacement ellipsoids, most H atoms are omitted). Selected distances (Å) and angles (deg) for (pR,R_p) -9: P1–F1 1.5851(10), P1–N1 1.6509(14), P1–B1 1.899(2), P1–C21 1.8303(17), C7–C8 1.348(2), F1–P1–N1 106.13(6), F1–P1–B1 109.60(7), F1–P1–C21 100.51(7), N1–P1–B1 112.98(8). For (pR,R_p) -10: P1–F1 1.6286(10), P1–N1 1.6805(12), P1–C21 1.8579(15), C7–C8 1.3540(18), F1–P1–N1 103.19(6), F1–P1–C21 97.10(6), N1–P1–C21 106.08(6).

R_p)-9, which confirms the formation of the P–F bond ($d_{P-F} = 1.585(10)$ Å), the absolute configuration of the P-atom, and the planar chirality of the dibenzooazepine ring, which are (pR,R_p) . Importantly, expensive $(-)$ -sparteine can be recycled quantitatively. The basicity of the P-donor in (pR,R_p) -9 seems lower than in (pR,R_p) -3,²⁴ because removal of the BH_3 moiety from (pR,R_p) -9 is achieved with NEt_3 , instead of DABCO affording diastereo- and enantiopure free fluorophosphinamide (pR,R_p) -10 in excellent yields. To make sure deprotection did not erode enantiopurity, (pR,R_p) -10 was re-protected with $BH_3\cdot THF$

giving back (pR,R_p) -9 in $> 99\%$ optical purity. ^{31}P and ^{19}F NMR spectra show new doublets at 176.7 ppm and -132.3 ppm, respectively, with $J_{PF} = 970.6$ Hz. In the ^{13}C NMR spectrum, the quaternary carbon and the methyl groups of the *tBu* moiety, appear at 35 ppm as a doublet of doublets at 35.0 ($J_{CP} = 25.3$ Hz, $J_{CF} = 12.1$ Hz) and 25.4 ppm ($J_{CP} = 19.5$ Hz, $J_{CF} = 1.7$ Hz), respectively. The crystal structure confirms the unaltered configuration in (pR,R_p) -10 and shows significant elongation of both the P–F (to 1.6286(10) Å) and P–N bonds compared with (pR,R_p) -9 (Fig. 2). Deprotected (pR,R_p) -9 is surpris-



ingly robust: It is air-stable in the solid state and withstands boiling chloroform and toluene solutions without showing signs of decomposition or epimerization.

(*pR,R_P*)-3 and (*pR,R_P*)-10 both react with $[\text{RhCl}(\text{COE})_2]_2$ (COE = cyclooctene) to form the respective P-alkene ligated dinuclear complexes (*pR,R_P*)-11 (see Fig. S1 in the SI for its crystal structure) and (*pR,R_P*)-12²⁵ according to eqn (1). The $^{31}\text{P}\{\text{H}\}$ spectrum of (*pR,R_P*)-12 shows the formation of a single isomer with a doublet of doublets centered at 231.5 ppm ($J_{\text{PF}} = 1066$ Hz, $J_{\text{PRh}} = 249.6$ Hz), and the non-decoupled ^{19}F spectrum exhibits a doublet of doublets at -104.8 ppm ($J_{\text{F-P}} = 1065$ Hz, $J_{\text{F-Rh}} = 16.4$ Hz). The alkene-C–H resonates at relatively low frequency as a singlet at

5.70 ppm, indicating alkene coordination. (*pR,R_P*)-12 crystallizes as red blocks from benzene solution, and its crystal structure in Fig. 3 confirms the bidentate coordination of the ligands in an *anti*-fashion to the Rh_2Cl_4 butterfly core, which spans an angle of 99° between the square coordination planes around the Rh atoms. The P–F bond is shorter than in the free ligand and is comparable to the P–F bond in borane complex 8. The P–F bond in complex (*pR,R_P*)-12 is significantly shorter than the P–Me bond in complex (*pR,R_P*)-11, measuring 1.58 vs. 1.82 Å, respectively (1.63 vs. 1.82 Å in the respective free ligands). Including the H-atoms of the methyl substituent an even larger difference in the respective van-der-Waals volumes is expected. Fluorine substitution at the P-donor also shortens

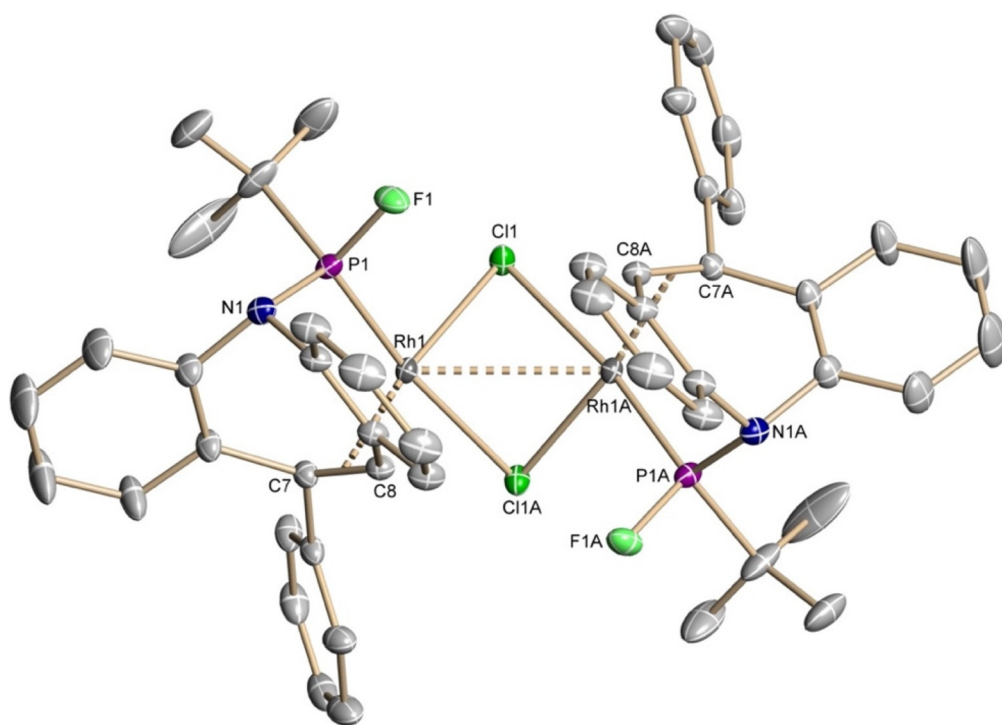
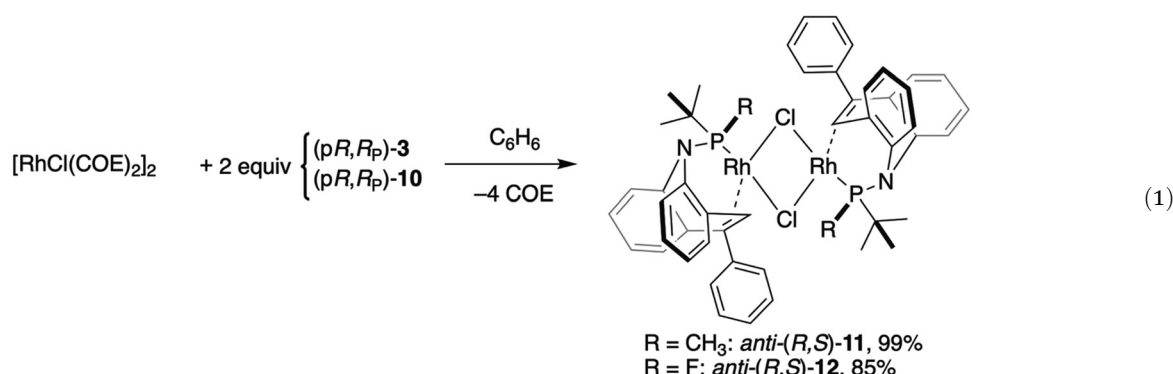


Fig. 3 Crystal structure of (*pR,R_P*)-12 (50% displacement ellipsoids, H atoms are omitted). Selected distances (Å) and angles (deg): Rh1–Cl1 2.3685 (3), Rh1–Cl1A 2.5010(3), Rh1–P1 2.132(4), Rh1–C7 2.1654(13), Rh1–C8 2.1107(13), C7–C8 1.4330(19), P1–F1 1.5845(10), P1–N1 1.7035(12), F1–P1–Rh1, 113.35(4), F1–P1–N1 98.17(6), F1–P1–C21 100.23(8)



the Rh-P bond in complex $(\text{p}R,\text{R}_\text{P})\text{-12}$ ($2.132(4)$ Å) compared to $(\text{p}R,\text{R}_\text{P})\text{-11}$ ($2.1622(9)$ Å); a small but statistically significant difference.

The P-F ligand $(\text{p}R,\text{R}_\text{P})\text{-10}$ was then benchmarked against ligands $(\text{p}R,\text{R}_\text{P})\text{-2}$ and $(\text{p}R,\text{R}_\text{P})\text{-3}$ of identical planar chirality in the base-free arylation of isatins with sodium tetraarylborates²⁶ to biologically important 3-aryl-3-hydroxyindoles (Table 1).²⁷ The arylation of benzyl-protected isatin **14a** with NaBPh_4 , is catalyzed by $(\text{p}R,\text{R}_\text{P})\text{-12}$ bearing the P-F ligand affords **16aa** quantitatively in 86% ee, whereas the previously reported cationic complex $[\text{Rh}((\text{p}R,\text{R})\text{-2})_2][\text{BF}_4]$ ^{12a} and $(\text{p}R,\text{R}_\text{P})\text{-11}$ bearing ligands $(\text{p}R,\text{R}_\text{P})\text{-2}$ and $(\text{p}R,\text{R}_\text{P})\text{-3}$, respectively, give conversions of $<10\%$. Only with the electron-poor isatin **14b** do these catalysts

afford relevant quantities of **16ba**. For this product, catalyst $(\text{p}R,\text{R}_\text{P})\text{-11}$ exhibits good enantioselectivity compared with the much more active but less selective $(\text{p}R,\text{R}_\text{P})\text{-12}$. The sense of induction of the ligands with the Me- and the F-substituted P-donors is identical.²⁸ *In situ* generation of the cationic catalyst $[\text{Rh}((\text{p}R,\text{R})\text{-10})_2][\text{NTf}]$ pushes the ee of the protected dimethyl hydroxyindole **16ca** up to 96%. Surprisingly, catalyst $(\text{p}R,\text{R}_\text{P})\text{-12}$ works even better with unprotected NH isatins²⁹ at reduced catalyst loadings. Electron-donating substituents at R^1 *para* to the NH function appear to favor enantioselectivity affording hydroxyindoles of very high enantiomeric purity (compounds **16fa**, **16ha** and **16ia**), while *N*-protection and the use of tetra-*p*-tolylborate **15b** significantly erode enantioselectivity.

Table 1 Benchmarking of ligand $(\text{p}R,\text{R}_\text{P})\text{-10}$ in the water- and base-free catalytic arylation of isatins with tetraarylborates

14a-i		15a, Ar = Ph $\text{15b, Ar = }p\text{-Tol}$		$2.5\text{--}1.5\text{ mol\% }\{\text{cat}\}$ Dioxane/CH ₃ OH (10/1) 45 °C, 18 h		16	
	$\{\text{(p}R,\text{R}_\text{P})\text{-12}\}$ 2.5 mol% Conv. 100% ee 86% (S)		$\{[\text{Rh}(\text{p}R,\text{R})\text{-2})_2][\text{BF}_4]\}$ 5 mol% Conv. 30% ee 5% (S)		$\{\text{(p}R,\text{R}_\text{P})\text{-11}\}$ 2.5 mol% Conv. 20% ee 80% (S)		$\{\text{(p}R,\text{R}_\text{P})\text{-12}\}^a$ 2.5 mol% Conv. 100% ee 71% (S)
	$\{\text{(p}R,\text{R}_\text{P})\text{-12}\}$ 2.5 mol% Conv. 100% ee 92%		$\{[\text{Rh}((\text{p}R,\text{R})\text{-10})_2][\text{NTf}]\}^b$ 5 mol% Conv. 100% ee 96%		$\{\text{(p}R,\text{R}_\text{P})\text{-12}\}$ 2.5 mol% Conv. 100% ee 91% (S)		$\{\text{(p}R,\text{R}_\text{P})\text{-12}\}$ 1.5 mol% Conv. 96% ee 93% (S)
	$\{\text{(p}R,\text{R}_\text{P})\text{-12}\}^c$ 1.5 mol% Conv. 100% ee 63%		$\{\text{(p}R,\text{R}_\text{P})\text{-12}\}$ 1.5 mol% Conv. 81% ee 98%		$\{\text{(p}R,\text{R}_\text{P})\text{-12}\}$ 1.5 mol% Conv. 100% ee 88%		$\{\text{(p}R,\text{R}_\text{P})\text{-12}\}^c$ 1.5 mol% Conv. 96% ee 89%
	$\{\text{(p}R,\text{R}_\text{P})\text{-12}\}$ 1.5 mol% Conv. 94% ee 87%		$\{\text{(p}R,\text{R}_\text{P})\text{-12}\}$ 1.5 mol% Conv. 80% ee 96%		$\{[\text{Rh}((\text{p}R,\text{R})\text{-10})_2][\text{NTf}]\}^b$ 5 mol% Conv. 89% ee 98.5%		$\{\text{(p}R,\text{R}_\text{P})\text{-12}\}$ 1.5 mol% Conv. 100% ee 99.5% (S)

^a Reaction performed at 35 °C for 4 d. ^b Catalyst formed *in situ* from $(\text{p}R,\text{R}_\text{P})\text{-12} + 2$ equiv. $(\text{p}R,\text{R}_\text{P})\text{-10} + 2$ equiv. AgNTf (for experimental details, see the SI). ^c Reaction performed with 1 equiv. of **15b**.



Conclusions

We report a significant advance in the long-standing synthetic challenge of preparing a stereochemically stable P-stereogenic fluorophosphines of the type $\text{PR}^1\text{R}^2\text{F}$. This was achieved *via* enantiospecific electrophilic fluorination of the crystalline alkene-phosphide ($\text{pR}_2\text{S}_\text{P}$)-7, yielding the configurationally stable fluorophosphinamide ($\text{pR}_2\text{R}_\text{P}$)-10 in gram quantities. This compound introduces a novel donor motif for chiral ligand design and functions as a bidentate ligand in the Rh(I) complex (pR_2R)-12. In rhodium-catalyzed, water- and base-free arylations of isatins using NaBAr_4 nucleophiles, ($\text{pR}_2\text{R}_\text{P}$)-10 performs favorably compared to benchmark planar-chiral ligands 2 and 3, particularly in the arylation of unprotected NH-isatins. This transformation marks the first application of a fluorophosphinamide in asymmetric catalysis. Notably in this context, the $\text{P}(t\text{-Bu})\text{F}$ synthon outperforms the generally effective $\text{P}^*(t\text{-Bu})(\text{Me})$ analog.¹³ Furthermore, the crystalline phosphide ($\text{pR}_2\text{S}_\text{P}$)-7 provides a versatile platform for accessing new classes of P-stereogenic P-alkene hybrid ligands, the exploration of which is currently underway.

Conflicts of interest

The authors declare no conflicts of interest.

Data availability

Synthetic procedures, X-ray crystallographic data, NMR spectra, and HPLC traces for this study are available as Supplementary Information. See DOI: <https://doi.org/10.1039/d5qi01994j>.

CCDC 2390089–2390093 contain the supplementary crystallographic data for this paper.^{30a-e}

Acknowledgements

We thank Ms Antigone Roth for carrying out the elemental analyses, Mr Shao Kai Lu for assistance in up-scaling the synthesis of ($\text{pR}_2\text{S}_\text{P}$)-7, and Mr Jochen Schmidt for measuring NMR spectra. Financial support by Friedrich-Alexander University is gratefully acknowledged.

References

- 1 A. B. Burg and G. Brendel, Fluorocarbon-Phosphinoborines and Related Chemistry, *J. Am. Chem. Soc.*, 1958, **80**, 3198–3202.
- 2 For reviews, see: (a) T. Kruck and M. Höfler, Synthesis of Tetrakis(trimethoxyphosphine)nickel(0), *Angew. Chem., Int. Ed. Engl.*, 1967, **6**, 563; (b) J. F. Nixon and J. R. Swain, Trifluorophosphine Complexes of the Platinum Metals, *Platinum Metals Rev.*, 1975, **19**, 22–29; (c) H.-R. Jaw and J. I. Zink, Angular-overlap interpretation of σ and π bonding of phosphorus trifluoride and phosphorus trichloride in platinum PtCl_3L complexes, *Inorg. Chem.*, 1988, **27**, 3421–3424.
- 3 For crystallographically characterized complexes of RPF_2 , see: (a) J. R. Goerlich, J.-V. Weiss, P. G. Jones and R. Schmutzler, *Phosphorus, Sulfur Silicon Relat. Elem.*, 1992, **66**, 223–243; (b) F. Delgado Calvo, V. Mirabello, M. Caporali, W. Oberhauser, K. Raltchev, K. Karaghiosoff and M. Peruzzini, *Dalton Trans.*, 2016, **45**, 2284 For crystallographically characterized complexes of R_2PF , see: (c) W. S. Sheldrick and O. Stelzer, Preparation, crystal and molecular structure of *trans*-dibromobis-[di(*t*-butyl)fluorophosphine]nickel(II), *J. Chem. Soc., Dalton Trans.*, 1973, 926; (d) L. Heuer and D. Schomburg, *t*Bu₂PF as a ligand in triosmium clusters, *J. Organomet. Chem.*, 1995, **495**, 53–59.
- 4 For a recent review see: (a) A. Miles-Hobbs, P. G. Pringle, J. D. Woollins and D. Good, Monofluorophos–Metal Complexes: Ripe for Future Discoveries in Homogeneous Catalysis, *Molecules*, 2024, **29**, 2368–2395 For applications in alkene hydroformylation, see: (b) N. Fey, M. Garland, J. P. Hopewell, C. L. McMullin, S. Mastroianni, A. Guy Orpen and P. G. Pringle, Stable fluorophosphines: predicted and realized ligands for catalysis, *Angew. Chem., Int. Ed.*, 2012, **51**, 118–122 Notable patents assigned to Eastman Chemical Company are: (c) T. A. Puckette and G. E. Struck, Hydroformylation process using phosphite–metal catalyst system, US5840647, 1998; (d) T. A. Puckette, Hydroformylation process for the preparation of glycolaldehyde, US7301054B1, 2007; (e) T. A. Puckette, Amido–Fluorophosphite Compounds and Catalysts, US8492593B2, 2013; A very recent application in cross-coupling is: (f) F. Flecken, A. Neyyathala, T. Grell and S. Hanf, A Bench-stable Fluorophosphine Nickel(0) Complex and Its Catalytic Application, *Angew. Chem., Int. Ed.*, 2025, **64**, e202506271.
- 5 R. Noyori, in *Asymmetric Catalysis in Organic Synthesis*, Wiley, 1994; *Asymmetric catalysis on Industrial Scale*, ed. H.-U. Blaser and H.-J. Federsel, Wiley-VCH, 2010.
- 6 (a) W. S. Knowles, Asymmetric hydrogenation, *Acc. Chem. Res.*, 1983, **16**, 106–112; (b) W. S. Knowles, Asymmetric hydrogenations (Nobel Lecture), *Angew. Chem., Int. Ed.*, 2002, **41**, 1998–2007 For a new synthetic route to DIPAMP, see: Z. S. Han, N. Goyal, M. A. Herbage, J. D. Sieber, B. Qu, Y. Xu, Z. Li, J. T. Reeves, J.-N. Desrosiers, S. Ma, N. Grinberg, H. Lee, H. P. R. Mangunuru, Y. Zhang, D. Krishnamurthy, B. Z. Lu, J. J. Song, G. Wang and C. H. Senanayake, Efficient asymmetric synthesis of p-chiral phosphine oxides via properly designed and activated benzoxazaphosphinine-2-oxide agents, *J. Am. Chem. Soc.*, 2013, **135**, 2474–2477; For P-stereogenic ligands used in industry *post* DIPAMP, see: (c) T. Imamoto, T. Oshiki, T. Onozawa, T. Kusumoto and K. Sato, P-chiral bis(trialkylphosphine) ligands and their use in highly enantioselective hydrogenation reactions, *J. Am. Chem. Soc.*, 1998, **120**, 1635–1636; (d) T. Imamoto, K. Sugita and K. Yoshida, An air-stable p-chiral phosphine ligand for highly enantio-



selective transition-metal-catalyzed reactions, *J. Am. Chem. Soc.*, 2005, **127**, 11934–11935; (e) K. Tamura, M. Sugiya, K. Yoshida, A. Yanagisawa and T. Imamoto, Enantioselective 1,2-Bis(tert-butylmethylphosphino)benzene as a Highly Efficient Ligand in Rhodium-Catalyzed Asymmetric Hydrogenation, *Org. Lett.*, 2010, **12**, 4400–4403; (f) T. Imamoto, K. Tamura, Z. Zhang, Y. Horiuchi, M. Sugiya, K. Yoshida, A. Yanagisawa and I. D. Gridnev, Rigid P-Chiral Phosphine Ligands with tert-Butylmethylphosphino Groups for Rhodium-Catalyzed Asymmetric Hydrogenation of Functionalized Alkenes, *J. Am. Chem. Soc.*, 2012, **134**, 11934–11935.

7 For reviews of stoichiometric and catalytic methods, see: (a) M. Dutartre, J. Bayardon and S. Jugé, Applications and stereoselective syntheses of P-chirogenic phosphorus compounds, *Chem. Soc. Rev.*, 2016, **45**, 5771–5794 Selected reports on catalytic routes to P-chiral compounds are: (b) X. Ye, L. Penga, X. Baoa, C.-H. Tan and H. Wang, Recent developments in highly efficient construction of P-stereogenic centers, *Green Synth. Catal.*, 2021, **2**, 6–18; (c) D. Glueck, Catalytic Asymmetric Synthesis of P-Stereogenic Phosphines: Beyond Precious Metals, *Synlett*, 2021, **31**, 875–884; C. Wang, Y.-H. Dai, Z. Wang, B. Lu, W. Cao, J. Zhao, G. Mei, Q. Yang, J. Guo and W.-L. Duan, Nickel-Catalyzed Enantioselective Alkylation of Primary Phosphines, *J. Am. Chem. Soc.*, 2021, **143**, 5685–5690; (d) X. Gu, X. Mo, W.-J. Bai, P. Xie, W. Hu and J. Jiang, Catalytic Asymmetric P–H Insertion Reactions, *J. Am. Chem. Soc.*, 2023, **145**, 20031–20040; (e) M. Formica, T. Rogova, H. Shi, N. Sahara, B. Ferko, A. J. M. Farley, K. E. Christensen, F. Duarte, K. Yamazaki and D. J. Dixon, Catalytic enantioselective nucleophilic desymmetrization of phosphonate esters, *Nat. Chem.*, 2023, **15**, 714–721; (f) O. Berger and J. L. Montchamp, A general strategy for the synthesis of P-stereogenic compounds, *Angew. Chem., Int. Ed.*, 2013, **52**, 11377–11380.

8 Excellent reviews are: (a) A. Grabulosa, *P-stereogenic Ligands in Enantioselective Catalysis*, RSC Catalysis Series, RSC Publishing, 2011; (b) G. Xu, C. H. Senanayake and W. Tang, P-chiral phosphorus ligands based on a 2,3-dihydrobenzo[*d*][1,3]oxaphosphole motif for asymmetric catalysis, *Acc. Chem. Res.*, 2019, **52**, 1101–1112; (c) P. Rojo, A. Riera and X. Verdaguer, Bulky P-stereogenic ligands. A success story in asymmetric catalysis, *Coord. Chem. Rev.*, 2023, **489**, 215192; (d) T. Imamoto, P-Stereogenic Phosphorus Ligands in Asymmetric Catalysis, *Chem. Rev.*, 2024, **124**, 8657–8739.

9 *Chiral Ligands: Evolution of Ligand Libraries for Asymmetric Catalysis*, ed. M. Diéguez, Taylor & Francis Group, 1st edn, 2021.

10 D. J. Grant, M. H. Matus, J. R. Switzer, D. A. Dixon, J. S. Francisco and K. O. Christe, Bond, dissociation energies in second-row compounds, *J. Phys. Chem. A*, 2008, **112**, 3145–3156.

11 (a) C. Defieber, M. A. Ariger, P. Moriel and E. M. Carreira, Iridium-Catalyzed Synthesis of Primary Allylic Amines from Allylic Alcohols: Sulfamic Acid as Ammonia Equivalent, *Angew. Chem., Int. Ed.*, 2007, **47**, 3139–3143; (b) A. Briceño and R. Dorta, *cis*-Dichloridobis{[(S)-N-(3,5-dioxa-4-phosphacyclohepta[2,1-a;3,4-a']dinaphthalen-4-yl]dibenz[b,f]azepin- κ P}palladium(II) deuterochloroform solvate, *Acta Crystallogr., Sect. E: Struct. Rep. Online*, 2007, **63**, m1718–m1719; (c) R. Mariz, A. Briceño, R. Dorta and R. Dorta, Chiral Dibenzazepine-Based P-Alkene Ligands and Their Rhodium Complexes: Catalytic Asymmetric 1,4 Additions to Enones, *Organometallics*, 2008, **27**, 6605–6613; (d) E. Drinkel, A. Briceño, R. Dorta and R. Dorta, Hemilabile P-Alkene Ligands in Chiral Rhodium and Copper Complexes: Catalytic Asymmetric 1,4 Additions to Enones, *Organometallics*, 2010, **29**, 2503–2514 For an optimized synthesis of 1, see: (e) A. Herrera, A. Linden, F. Heinemann, R.-C. Brachvogel, M. von Delius and R. Dorta, Optimized Syntheses of Optically Pure P-Alkene Ligands; Crystal Structures of a Pair of P-Stereogenic Diastereomers, *Synthesis*, 2016, **48**, 1117–1123.

12 (a) L. Leinauer, G. Parla, J. Messelbeger, A. Herrera, F. W. Heinemann, J. Langer, I. Chuchelkin, A. Grasruck, S. Frieß, A. Chelouan, K. Gavrilov and R. Dorta, Evolution of a ‘privileged’ P-alkene ligand: added planar chirality beats BINOL axial chirality in catalytic asymmetric C–C bond formation, *Chem. Commun.*, 2023, **59**, 14451–14454 Energy barriers for the flipping of the dibenzazepine moiety in compounds such as 2 and *rac*-3 have been calculated to exceed 30 kcal mol⁻¹; (b) J. C. Calderón, A. Herrera, F. W. Heinemann, J. Langer, A. Linden, A. Chelouan, A. Grasruck, R. Añez, T. Clark and R. Dorta, Stereochemical stability of planar-chiral benzazepine tricyclics: inversion energies of P- and S-alkene ligands, *J. Org. Chem.*, 2023, **88**, 16144–16154.

13 E. Salomó, S. Orgué, A. Antoni Riera and X. Verdaguer, Efficient Preparation of (S)- and (R)-tert-Butylmethylphosphine–Borane: A Novel Entry to Important P-Stereogenic Ligands, *Synthesis*, 2016, **48**, A–E, and references cited therein.

14 *rac*-3 is synthesized by methylation of the diastereopure chloride precursor *rac*-4 (shown in Scheme 1) with MeLi: A. Herrera, A. Grasruck, F. W. Heinemann, A. Scheurer, A. Chelouan, S. Frieß, F. Seidel and R. Dorta, Developing P-stereogenic, planar-chiral P-alkene ligands: monodentate, bidentate, and double agostic coordination modes on Ru(II), *Organometallics*, 2017, **36**, 714–720.

15 M. Pabel, A. C. Willis and S. B. Wild, First resolution of a free fluorophosphine chiral at phosphorus. Resolution and reactions of free and coordinated (±)-fluorophenylisopropylphosphine, *Inorg. Chem.*, 1996, **35**, 1244–1249.

16 (a) M.-L. Y. Riu, R. L. Jones, W. J. Transue, P. Müller and C. C. Cummins, Isolation of an elusive phosphatetrahedrane, *Sci. Adv.*, 2020, **6**, eaaz3168; (b) P. M. Miura-Akagi, T. W. Chapp, W. Y. Yoshida, G. P. A. Yap, A. L. Rheingold, R. P. Hughes and M. F. Cain, Synthesis and structure of P-halogenated benzazaphospholes and their reactivity toward Pt(0) sources, *Organometallics*, 2023, **42**, 672–688.

17 (a) B. Wolfe and T. Livinghouse, A direct synthesis of P-chiral phosphine-boranes via dynamic resolution of lithiated racemic *tert*-butylphenylphosphine-borane with (-)-sparteine, *J. Am. Chem. Soc.*, 1998, **120**, 5116–5117.

18 G. Müller and J. Brand, Mono(borane)phosphides as ligands to lithium and aluminum, *Organometallics*, 2003, **22**, 1463–1467.

19 For an in-depth study of crystallization-induced dynamic resolution of a tertiary phosphine with an inexpensive chiral amine, see: M. Y. Kuzu, A. Schmidt and C. Strohmann, Enantioselective Synthesis of Phosphine Boranes via Crystallization-Induced Dynamic Resolution of Lithiated Intermediate by Understanding the Underlying Epimerization Process, *Angew. Chem., Int. Ed.*, 2024, **63**, e202319665.

20 B. Freitag, H. Elsen, J. Pahl, G. Ballmann, A. Herrera, R. Dorta and S. Harder, s-Block Metal Dibenzooazepinate Complexes: Evidence for Mg–Alkene Encapsulation, *Organometallics*, 2017, **36**, 1860–1866.

21 T. Imamoto, Y. Saitoh, A. Koide, T. Ogura and K. Yoshida, Synthesis and Enantioselectivity of P-Chiral Phosphine Ligands with Alkynyl Groups, *Angew. Chem., Int. Ed.*, 2007, **46**, 8636–8639.

22 (a) E. Differding and H. Ofner, *N*-fluorobenzenesulfonimide: a practical reagent for electrophilic fluorinations, *Synlett*, 1991, 187–189; (b) E. Differding, R. O. Duthaler, A. Krieger, G. M. Rüegg and C. Schmit, Electrophilic fluorinations with *N*-fluorobenzenesulfonimide: convenient access to α -fluoro- and α,α -difluorophosphonates, *Synlett*, 1991, 395–396.

23 As pointed out by a reviewer, the planar-chiral phenyl dibenzooazepine ring in phosphide (*pR,S_P*)-7 might play a role in the stereoselective addition of the electrophiles.

24 The basicity of fluorophosphines resembles that of phosphites and phosphoramidites.

25 Please note that the stereochemical descriptors in these complexes have been maintained (according to the CIP rules they should read *S_P*).

26 For a pioneering report, see: (a) R. Shintani, Y. Tsutsumi, M. Nagaosa, T. Nishimura and T. Hayashi, *J. Am. Chem. Soc.*, 2009, **131**, 13588–13589 For non-asymmetric additions of tetraarylborates to aldehydes and enones, see: (b) R. A. Batey, A. N. Thadani and D. V. Smil, *Org. Lett.*, 1999, **1**, 1683–1686, and to isatin in the presence of base, see: (c) C. Marques and A. Burke, Enantioselective Rhodium(i)-Catalyzed Additions of Arylboronic Acids to N-1,2,3-Triazole-Isatin Derivatives: Accessing N-(1,2,3-Triazolmethyl)-3-hydroxy-3-aryloxindoles, *ChemCatChem*, 2016, **8**, 3518–3526.

27 For a reviews, see: (a) K. Xie, A. Li, B. R. Konga, Z. C. Chen, W. Dua and Y. C. Chen, Recent Advances in Asymmetric Addition Reactions to Isatins, *Synthesis*, 2024, **56**, A–P; (b) B. Yu, H. Xing, D.-Q. Yu and H.-M. Liu, Catalytic asymmetric synthesis of biologically important 3-hydroxyoxindoles: an update, *Beilstein J. Org. Chem.*, 2016, **12**, 1000–1039.

28 Literature with unambiguous assignations of the absolute stereochemistry of 3-hydroxy-3-aryloxindoles is quite scarce (see SI). The determination of their absolute stereochemistry, along with DFT-modelling of enantio-determining steps, are the subjects of ongoing investigations in our laboratory.

29 (a) J. Gui, G. Chen, P. Cao and J. Liao, Rh(i)-catalyzed asymmetric addition of arylboronic acids to NH isatins, *Tetrahedron: Asymmetry*, 2012, **23**, 554–563; (b) X. Feng, Y. Nie, L. Zhang, J. Yang and H. Du, Rh(i)-catalyzed asymmetric 1,2-additions of arylboronic acids to isatins with chiral sulfur–alkene hybrid ligands, *Tetrahedron Lett.*, 2014, **55**, 4581–4584; (c) N. Saleh, C. Besnard and J. Lacour, Concave P-Stereogenic Phosphorodiamidite Ligands for Enantioselective Rh(i) Catalysis, *Org. Lett.*, 2024, **26**, 2202–2206.

30 (a) CCDC 2390089: Experimental Crystal Structure Determination, 2025, DOI: [10.5517/ccdc.csd.cc2l72nl](https://doi.org/10.5517/ccdc.csd.cc2l72nl); (b) CCDC 2390090: Experimental Crystal Structure Determination, 2025, DOI: [10.5517/ccdc.csd.cc2l72pm](https://doi.org/10.5517/ccdc.csd.cc2l72pm); (c) CCDC 2390091: Experimental Crystal Structure Determination, 2025, DOI: [10.5517/ccdc.csd.cc2l72qn](https://doi.org/10.5517/ccdc.csd.cc2l72qn); (d) CCDC 2390092: Experimental Crystal Structure Determination, 2025, DOI: [10.5517/ccdc.csd.cc2l72rp](https://doi.org/10.5517/ccdc.csd.cc2l72rp); (e) CCDC 2390093: Experimental Crystal Structure Determination, 2025, DOI: [10.5517/ccdc.csd.cc2l72sq](https://doi.org/10.5517/ccdc.csd.cc2l72sq).

